

Chapter 9

Phantoms for Ultrasound

Experimentation and Quality Control

Evan J. Boote

9.1 Background

Phantoms used in ultrasound were born out of a need for models of human anatomy and tissue characteristics. Initial ultrasound phantom construction was based on containers filled with water and would be constructed with metal rods at specific locations in order to provide a distance calibration. As ultrasound equipment became more sophisticated and advanced, it was recognized that a better material was needed to provide a medium for transmission of sound at the correct speed, to have reflectors that cause an echo to be returned to the transducer, while providing an attenuation of sound that is similar to that of experienced by sound waves in tissue. Hence, as is the case with many imaging modalities, the development of ultrasound phantoms has been driven by the progressively improved specifications of ultrasound imaging equipment [1].

Various materials, such as urethane polymers or soft plastics, were initially analyzed as possible media for phantom construction; however, these materials were deficient in one more of the physical parameters of ultrasound. The earliest report of materials designed to mimic tissue characteristics was published by a group at the University of Wisconsin–Madison [2, 3]. The methods of tissue-mimicking gel production developed from this work has served as the basis for many subsequent ultrasound phantoms. In the remainder of this chapter, the term “tissue mimicking” will be abbreviated by the initials “TM.”

Ultrasound phantom design and construction was also a part of the UW ultrasound group’s early work, always with application toward ultrasound quality control [4], but also, to provide an experimental platform for a better understanding of ultrasound physics and how imaging performance is related to the propagation of ultrasound in tissues [5, 6]. Anthropomorphic phantoms have been

E. J. Boote (✉)
Spectrum Health, Grand Rapids, MI, USA
e-mail: Evan.Boote@spectrumhealth.org

constructed and applied as part of a quality assurance program for a large, multi-center breast ultrasound study [7].

Contributions to ultrasound phantom development have also come from a number of ultrasound research laboratories, including the FDA [8], and research groups in Great Britain [9], the Netherlands [10], France [11, 12], Germany [13, 14], and Canada [15, 16]. While many of these have been built to provide a means to analyze the performance of imaging systems, a number of other phantoms are constructed for experiments to measure attenuation [17], backscatter [18–20], ultrasound exposimetry [21], and more recently, bulk material characteristics [22]. The latter types serve as “gold standards” to verify that the ultrasound techniques being used to measure tissue properties are indeed valid.

In addition to the laboratory development, a number of commercial vendors manufacture and market ultrasound phantoms for ultrasound quality control and training. With the worldwide market for ultrasound equipment is approaching \$5 billion per year with about a 5 % growth rate [23], these vendors have a large and growing market for a wide variety of quality assurance phantoms. Some designs are based on or developed from standards developed by national and international committees concerning ultrasound image quality. For example, the Technical Standards Committee of the American Institute of Ultrasound in Medicine has published descriptions of phantoms that have been produced by commercial vendors. In particular, the International Electrotechnical Commission, Group 87 has produced documents that describe phantoms and testing procedures for diagnostic ultrasound equipment [24, 25]. However, most of the commercial phantoms available today are built with unique designs made by a vendor based upon some common elements required for ultrasound quality control; these include a scanning/acoustic window, regularly spaced reflectors, and a background with a given sound speed and attenuation properties. Figure 9.1 shows images from several commercial vendors.

In addition to these, various methods have been published to fabricate “in-house” phantoms for various teaching and position equipment verifications. These range from a mixture of water and cornstarch [26], to mixtures of store-bought gelatin and psyllium hydrophilic mucilloid fiber [27]. The advantage of these phantoms is the low cost and ease of acquisition [28], albeit without absolute verification of the acoustic properties.

The objective of this chapter is to provide the reader with some basic parameters that are required for ultrasound phantoms, both for quality control of ultrasound as well as physical measurement standards. In addition, the design features of a basic ultrasound image quality control phantom will be considered as well as some specialized applications and the manner in which phantom design changes to accommodate these requirements. Lastly, the ongoing development and future trends in ultrasound phantoms will be discussed.

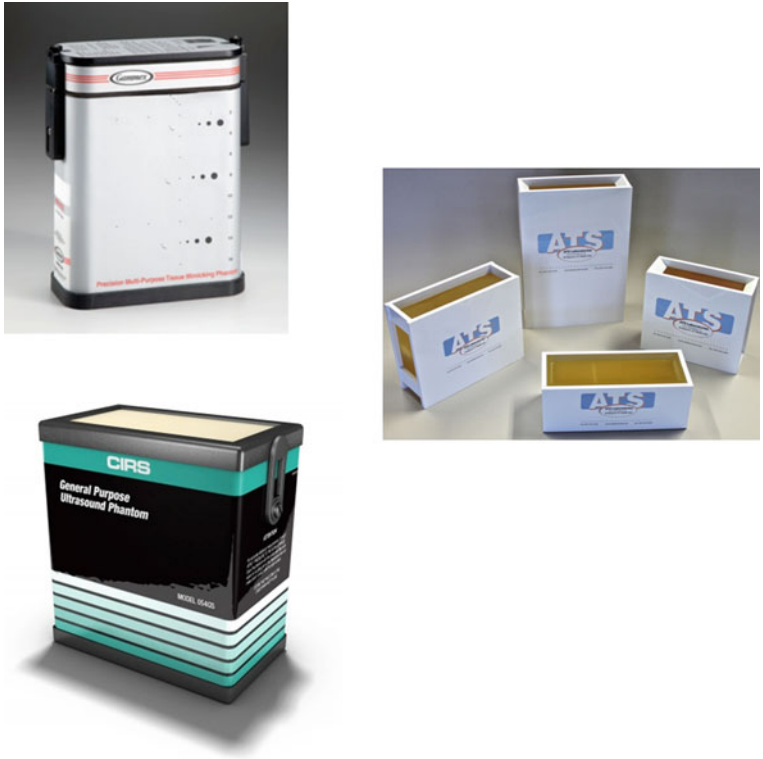


Fig. 9.1 Examples of commercially available ultrasound phantoms

9.2 Physical Parameters Required for Ultrasound Phantoms

The fact that the physical basis for ultrasound imaging is rather complex (compared to radiographic imaging) leads to the necessity of accurate physical parameters in ultrasound phantoms used for image quality measurements. Three key parameters are necessary for a proper ultrasound phantom, (1) sound speed, (2) attenuation and the frequency dependence of attenuation and (3) scattering. Other physical parameters, such as the density, non-linear parameter (B/A), are of some importance, but not always regarded as critical to a successful tissue mimic [28]. For obvious reasons, these parameters become more critical when the phantom is to be used as a standards model in an acoustics experiment. In some cases, e.g., for TM blood, the non-Newtonian fluid characteristics of human blood are impossible to mimic and therefore blood flow patterns are not precisely reproduced in Doppler phantoms vessels [29].

These physical properties should be applicable over the frequency range of most clinical diagnostic ultrasound systems (2–15 MHz). In response to the development

Table 9.1 Acoustic parameters for various tissues (several sources)

Tissue/Material	Velocity (m s ⁻¹)	Attenuation (dB cm ⁻¹ MHz ⁻¹)	Density (kg m ⁻³)	Acoustic impedance (MRayl)	Backscatter coefficient (10 ⁻⁴ cm ⁻¹ sr ⁻¹)
Air	330		1.2	0.0004	
Water	1,480	0.0022	1,000	1.48	
Soft tissue (average)	1,540	0.3–0.8	1,043	1.63	
Muscle	1,547–1,600	0.2–0.6	1,050	1.62	
Blood	1,560–1,584	0.2	1,060	1.68	0.1–1
Breast	1,510	0.75	1,020	1.54	
Liver	1,555–1,595	0.4–0.7	1,060	1.69	1–25
Cardiac	1,576	0.52	1,060	1.67	
Fat	1,450–1,480	0.5–1.8	950	1.40	

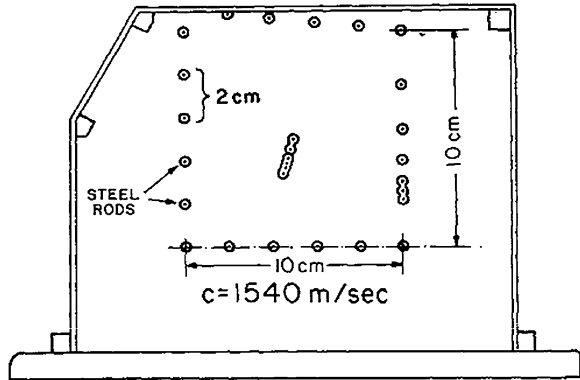
of higher-frequency probes for higher resolution imaging (preclinical at 20 MHz and above) have resulted in characterization of agar-based ultrasound phantoms at these frequencies [30–32].

Table 9.1 provides a range of typical compressional sound speed, density, and acoustic attenuation for a set of tissues. Sound speed and attenuation are the easiest parameters to verify and control and thus are regarded to be well-controlled in commercially available phantoms. Acoustic scattering, quantified by the backscatter coefficient (differential scattering cross section per unit volume) is a more difficult parameter to measure. Desirable characteristics for ultrasound phantom materials not only include these acoustic parameters, but also stability (thermal and temporal), low cost, and ease of manufacture.

9.2.1 Sound Speed (Density and Acoustic Impedance)

As mentioned at the beginning of this chapter, early ultrasound phantoms were typically built as plexiglass containers that were filled with water to provide a transmission medium for sound. As water is the simplest tissue substitute, this was an inexpensive alternative. One of the earliest of these types was the AIUM-type 100 ultrasound phantom (Fig. 9.2) [33]. Reflectors placed at fixed “depths” in the phantom produced echoes that would be registered on the ultrasound images and evaluated to determine correct distance calibration. This was important for early ultrasound units, which commonly required adjustment to insure that the depth calibration based on round trip time was correct. The reflectors were placed at depths that were adjusted so that the phantoms were built to “mimic” the sound speed of tissue ($c = 1.54\text{mm}/\mu\text{s}$) even though the sound speed of water is about 4 % slower ($1.48\text{mm}/\mu\text{s}$). Later phantoms were built with reflectors placed at the proper depths, and the sound speed of the fluid medium was increased by adding alcohol to water. The addition of 7.4 % ethanol to water increases the sound speed to $1,540\text{m s}^{-1}$.

Fig. 9.2 The AIUM 100 mm ultrasound test object



One of the disadvantages of water-based phantoms is there is a strong temperature dependence of the sound speed in water. Lubbers [34] provides a simple equation for the compressional sound speed in water over an interval of 15°–35° C:

$$c = 1404.3 + 4.7 T - 0.04 T^2 \tag{9.1}$$

Though it is a simple, easily obtained acoustic medium, water is insufficient for ultrasound phantoms requiring accurate sound speeds. Soft tissue substitutes having more accurate and stable sound speeds are desirable for use with imaging systems. Other tissue substitutes are typically based on gelatins, agarose, or other materials based on organic hydrocarbon-based chains. Some commercially marketed phantoms are constructed from urethane rubber; these offer stability in sound speed, but have a lower density and sound speed than soft tissue. Targets in these urethane phantoms are adjusted to “mimic” a phantom having a sound speed of 1,540 m s⁻¹.

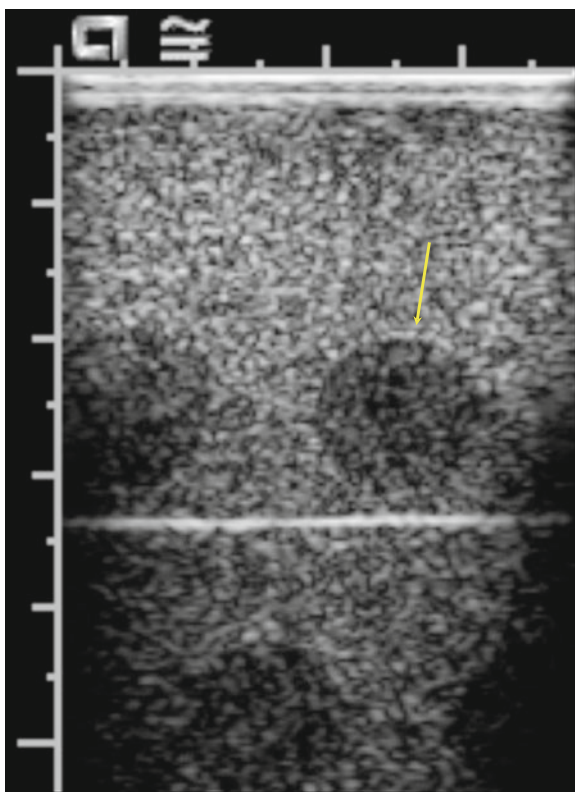
Many TM-gel-based phantoms are made from gelatin or agarose and are formulated to have a sound speed that is within 2 % of the sound speed of soft tissue (1,540 m s⁻¹). This can be accomplished by the addition of n-propanol alcohol [2], evaporated milk [35], or glycerol [36]. Reproducible and stable sound speed and density at room temperatures have been achieved through the use of these materials. Longevity is another issue with gelatin phantoms; this has been mitigated by adding antimicrobial agents into the gel and sealing the phantom well to prevent desiccation.

Layers of subcutaneous fat are often encountered in the transmit–receive ultrasound paradigm, and in some cases, the simulation of these fat layers are important to mimic the “true” conditions encountered by the beam as it passes through these layers [37]. In order to evaluate the effect of these sound speed, acoustic impedance boundaries, and varying attenuation layers on the performance of multi-element transducers, layers (sometimes with varying thicknesses) of fat simulating material are interposed between the scanning surface and the parenchyma mimic. Safflower oil is typically used as a substitute for subcutaneous fat [38]. Methods to incorporate these fat substitutes in oil-dispersed gelatin molds have been described, resulting in materials with sound speeds (1,491 m s⁻¹) and attenuation and scattering characteristics similar to that of human fat.

The importance of proper control of sound speed and density in gel-based phantoms must be emphasized here, especially in phantoms built to provide low-contrast imaging targets. Because acoustic reflection at an interface is related to the acoustic impedance ($Z = \text{velocity} \times \text{density}$), any small differences at an interface will produce an echo that is registered in the ultrasound image. Having such a readily visible interface defeats the purpose of placing low-contrast objects within a background as the targets are quite easily discerned by this bright echo that appears on the ultrasound image. Commercial vendors strive to make these acoustic impedance differences as small as possible. Figure 9.3 is an example of a low-contrast test object with a slight impedance mismatch; this shows up as a bright echo at the perpendicular interface between the acoustic beam and the border between the background and the object.

With the widespread adoption of harmonic imaging, the non-linearity parameter (B/A) has become of somewhat greater importance [39]. B/A is a non-dimensional value that expresses the degree to which the density (and hence sound speed) changes in a material with respect to the pressure amplitude. These pressure-dependent changes thus produce increasing propagation in compression and decreasing propagation speed in rarefaction, converting sine wave into sawtooth

Fig. 9.3 The arrow points to a very slight acoustic impedance mismatch between the background of the phantom and the low-contrast (*lower echogenicity*) object. This may lead to a false impression of the presence of an object



and resulting in the generation of harmonics. In harmonic imaging mode, an ultrasound system using a broad-frequency response transducer sends pulses at a lower frequency, but “tunes” to receive echoes centered at two times this frequency. A phantom with a tissue-like B/A (reported to be equal to around 7 for soft tissues) will demonstrate and test harmonic imaging reliably.

Gelatin-based phantoms have another advantage over liquid-based media in that the incorporation of other particles and materials to achieve tissue-like attenuation and scattering within the phantom.

9.3 Attenuation

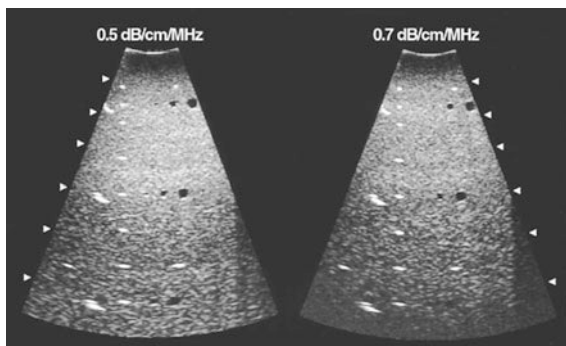
Attenuation is a very important property for phantoms used to evaluate the performance of ultrasound imaging systems. This is due to the fact that the attenuation of the sound energy in the pulse–echo mode is compensated for by time-gain compensation (TGC). Furthermore, the formation of the ultrasound image in a state-of-the-art ultrasound system is a complex process that at times involves multiple transmit beams and image reconstruction and sophisticated image processing that takes into account the expected attenuation that occurs during anatomical imaging. Acoustic attenuation increases roughly linearly with frequency, which means that (a) different frequency probes will result in widely varying attenuation, and (b) systems designed to achieve broad-band frequency response will exhibit different results if the ultrasound phantom does not have tissue-like attenuation properties.

As seen in Table 9.1, the attenuation of soft tissue varies widely, but is usually approximated as being linear with frequency. Attenuation is expressed in decibels per unit length (typically cm) and normalized by frequency. For example, if the attenuation is 3 dB cm^{-1} and the frequency is 5 MHz, then the attenuation is $0.6 \text{ dB cm}^{-1} \text{ MHz}^{-1}$. For soft tissue mimics, the target attenuation is between 0.5 and $0.7 \text{ dB cm}^{-1} \text{ MHz}^{-1}$. A non-linear attenuation response (f^n , $n > 1$) will result in higher attenuation at higher frequencies than what would be encountered in soft tissues. This may produce test results that show degraded performance for higher-frequency transducers [37].

Acoustic attenuation is achieved in gel-based phantom materials through the introduction of graphite powder [2], evaporated milk [35], Al_2O_3 [40], and by PMMA microsphere [41]. For the microspheres, the dominant mechanism contributing to attenuation is scattering. However, soft tissues are a weakly scattering medium, e.g., attenuation is not dominated by scattering. In addition, scattering is not linear with frequency, due to Rayleigh and Mie scattering, depending upon the ultrasound frequency. Therefore, the high number density microsphere approach is not as desirable to produce attenuation coefficients that scale linearly with frequency.

Most of the commercially available phantoms are constructed to have either 0.5 or $0.7 \text{ dB cm}^{-1} \text{ MHz}^{-1}$. In some cases, the higher attenuation value is used to provide a more strenuous test of system sensitivity, particularly at the lower

Fig. 9.4 An example of the effect of attenuation. These images are acquired with the same ultrasound configuration; the phantom on the left has lower attenuation. The brighter appearance beyond 8 cm depth is due to less signal loss at depth



frequencies. This reduces the required size and weight of a phantom, yet still provides the ability to determine a maximum depth of penetration around 2.5 MHz. Another approach taken is to have two sections of the phantom, one with $0.5 \text{ dB cm}^{-1} \text{ MHz}^{-1}$ and one with $0.7 \text{ dB cm}^{-1} \text{ MHz}^{-1}$ (Fig. 9.4).

9.4 Scattering

Acoustic scattering in ultrasound is the result of small-scale (size of the wavelength and smaller) inclusions of varying acoustic impedance [42]. Scattering is dependent upon the acoustic impedance, the size and shape of the scattering object, and the frequency of the sound [43]. For a volume of scatterers, one typically refers to the “backscatter coefficient,” which is the degree of scattering per unit volume. This value will vary according to the differential scattering cross section per “scatterer” and the density of scatterers (N per cm^3). The backscatter coefficient expressed in dimensions of $\text{cm}^{-1} \text{ sr}^{-1}$ and for soft tissues is in the range of 10^{-3} – 10^{-4} and between 10^{-4} and 10^{-5} for blood.

Many of current commercial phantoms incorporate 20–80 micron diameter glass beads at appropriate concentrations to achieve a backscatter coefficient that approximates liver tissue [20]. While the acoustic impedance difference of glass beads and the background gels is considerably more significant than tissue acoustic impedance differences, the number of scatterers per unit volume is adjusted accordingly. Similarly, objects of varying contrast can be made by changing the concentration of scatterers. This is typically done on the decibel scale, e.g., -6 or $+3$ dB.

Because the statistics of scattering are affected by the scatterer density [44], the diameter of the scatterers must be small enough and number density of scatterers must be large enough to provide sufficient statistical variation to demonstrate ultrasound speckle. As is the case with backscatter coefficient, many TM phantom materials aim to mimic liver tissue in this regard.

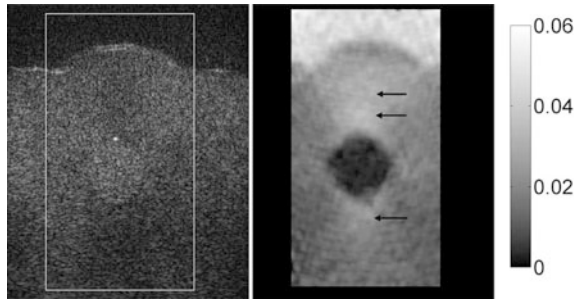


Fig. 9.5 An example of a phantom with an inclusion simulating a fibroadenoma. A standard B-mode image is on the left; the right side is an elastogram. For the image on the right, the bright region at the top of the image corresponds to softer TM fat while the harder TM fibroadenoma is the dark region in the center of the image

9.5 Mechanical Properties

More recently, the mechanical (viscoelastic) properties of ultrasound phantoms must be considered. These have become important since the introduction of methods which analyze ultrasound echo signals to under varying degrees of compression [45, 46], or, alternatively through the use of acoustic radiation force [47, 48]. Phantoms serve as useful means by which these methods are tested, both in the laboratory as the algorithms are developed as well as a way to check the contrast display performance for elastography applications on clinical equipment. Oil-in-gelatin-based phantoms have been developed to mimic this property of tissue, with a Young's modulus value of between 6 and 12 kPa. Harder (more stiffness) objects are typically present as inclusions in the background, with the same sound speed, attenuation, and scattering; these are used to evaluate the effectiveness of the algorithm by providing a comparison of the backscatter image alongside the elastography image (see Fig. 9.5). The challenge is to maintain all of the other acoustic characteristics as constant while varying the Young's modulus.

9.6 Multi-Modality Phantoms Based on TM Gels

From the earliest days of CT and ultrasound as complimentary modalities, individuals have attempted to utilize phantoms that could be applied to both [49] modalities. Acoustic tissue models based on organic materials offer similar X-ray attenuation characteristics as soft tissues. It is not difficult to incorporate other (higher atomic number) structures into the gel phantoms. In addition, it is also possible to dope the same aqueous gels used for ultrasound phantoms with paramagnetic salts to obtain tissue-like magnetic resonance properties (T1 and T2) [50]. This eventually resulted in the construction of a prostate mimic that could be

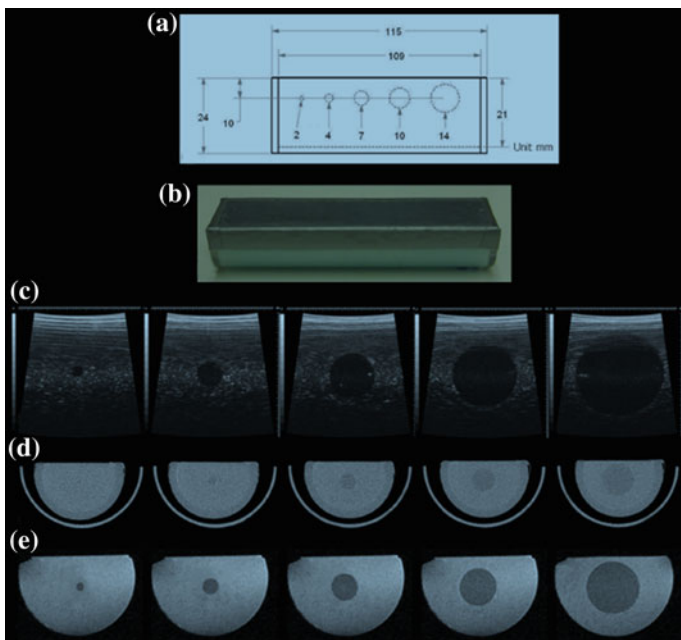


Fig. 9.6 An example of a multimodality phantom with ultrasound (*top row*), computed tomography (*middle row*) and magnetic resonance imaging (*bottom row*) systems used for preclinical imaging (need permission from Lee, Fullerton, etc., UTHSA)

used for ultrasound, CT, and MRI [51]. Another set of phantoms has been produced by a collaboration between a commercial vendor and a university laboratory [52]. These phantoms are designed to determine the accuracy of volume measurements for preclinical imaging systems and are compatible with US, CT, and MRI.

Other phantoms have been constructed for determination of proper safety checks for therapeutic applications of ultrasound. These have been used in high-intensity-focused ultrasound (HIFU) therapy applications under guidance by MRI [53]. Another “liver” ultrasound phantom has been applied to identify spatial errors in surgical navigation systems [54]. As ultrasound imaging continues to evolve into an imaging and therapeutic modality, many more phantom configurations and applications could result (Fig. 9.6).

9.7 Applications of Phantoms in Ultrasound

Ultrasound phantoms constructed as test tool measurement standards are often custom-built with the measurement device requirements in mind. Most common methods for sound speed, attenuation, and backscatter measurements involve

immersion in water baths to control temperature and to provide a coupling medium to acoustic transducers. If produced using gelatin-based recipes, the phantoms are typically cast inside a box or cylinder of plexiglass, then are covered with a thin layer of plastic [55]. The immersion experiment is conducted with a parallel beam interface to the acoustic beam. With two parallel acoustic “windows,” the phantom may be used for through transmission (sound speed and attenuation) and for pulse–echo (backscatter) measurements.

The additional parameters (non-linearity, mechanical stiffness) become more important when the objective of the phantom is to become a standard test object for validation of measurement methods and algorithms.

Another manner in which ultrasound phantoms are used for teaching and training. Ultrasonographers are required to understand and know the underlying anatomy and its appearance as they perform studies. Anthropomorphic phantoms are intended to provide a reusable and repeatable, if not quite realistic, way to provide the trainee with the experience of placing the ultrasound probe on the correct part of the body, locating the anatomy of interest and then to optimize and capture the images required for the study. In some instances, these phantoms are recognizable in the mannequin-like appearance; other types are only small portions of the body or are (for endocavitary transducers) enclosed within a box with an opening for insertion of the transducer [56]. Another type models the fetus at different stages of development (Fig. 9.7).

Additionally, training phantoms are useful when an operator is training to perform needle-based biopsy procedures where ultrasound imaging is used for guidance. The development of operator hand-eye coordination and muscle memory is the objective of these phantoms. One of the more common of these types are cast in the shape of a breast and have “cysts” and “lesions” embedded within as targets for drainage or

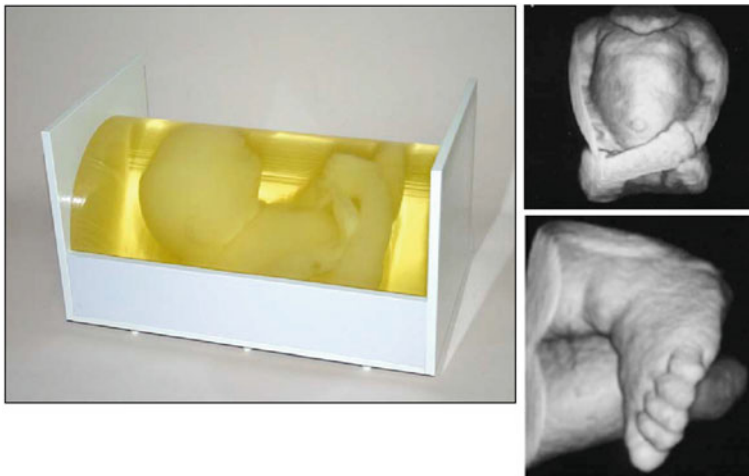


Fig. 9.7 An example of an anthropomorphic phantom; simulating an in-utero fetus

biopsy, respectively. Another category of these phantoms are used for training physicians to perform peripheral nerve blocks under ultrasound guidance. These phantoms include a TM background, artery and vein (collapsible) simulated by tubing, TM bone, TM muscle, and hyper- and hypo-echoic TM nerve bundles.

With ultrasound use proliferating beyond the radiology department (and other “traditional” ultrasound users such as obstetrics, vascular, and cardiac), the demand for these teaching and training phantoms can only increase. While ultrasound has typically relied upon human volunteers for teaching and training, the more invasive procedures preclude the use of volunteers.

Finally, the most common application for ultrasound phantoms is for verification of imaging system performance. In addition, verification of Doppler ultrasound system performance is also useful with specially designed ultrasound phantoms. These aspects will be considered in more detail in the following sections.

9.8 Image Quality Control

As stated at the beginning of the chapter, ultrasound phantom development has been driven by the need to evaluate the performance of ultrasound imaging equipment. While it seems rather obvious, it needs to be stated that phantom design and construction is dictated by the types of tests that are to be performed [57].

For ultrasound imaging, the development of new technology has outpaced the development of phantoms; imaging system vendors are in a competitive race to bring to market the best spatial and contrast resolution possible. At times, these systems have exceeded the characteristics of the phantom. Ultrasound imaging, while on the surface seemingly simple, is in reality a very complex process; consider the formation of a beam by a set of transducer elements, over a wide band of frequencies at a single depth or multiple depths. The acoustic energy is attenuated and scattered—the received echoes are “focused” again by a set of delays on the transducer elements and the signal is amplified (time-dependent to correct for attenuation) and processed by another complex set of algorithms that threshold, logarithmically transform, and envelope detect. If operating in harmonic mode, the RF signal is filtered to remove the fundamental frequency and retain only the first harmonic. Images are reconstructed from a set of acoustic lines that are recorded differently for transducer types, for example, linear versus curvilinear arrays. Add to this complexity the possibility of multi-dimensional (1.25x, 1.5x, and 2x transducer arrays) and multiple shapes and frequencies of transducers. The image that is formed by a set of acoustic lines also undergoes image processing to establish the gray scale and reduce speckle.

This leads to a wide variety of phantom designs and applications, aimed at testing differing aspects of imaging system performance; it is beyond the scope of this text to report on all of these, so the focus here will be on basic imaging system quality control. The principle tests that are usually expected in the course of ultrasound imaging QC are distance calibration, sensitivity, uniformity, and resolution (spatial and contrast) [58].

Distance calibration determination is achieved by placed fixed targets at specific depths within the TM material. These are typically narrow nylon fibers which are imaged in cross section (the image plane perpendicular to the direction of the fiber run). Cursors are placed on the image and a comparison is made between the known distance and the measured distance. In most cases, an accuracy determination is made in both the axial (beam direction) as well as the lateral direction. An extension of this test would be to determine the accuracy of the area determination for a single slice or, in the case of a three-dimensional ultrasound imaging protocol, the volume measurement accuracy.

Sensitivity is a measure of the ability of the ultrasound instrument to detect and display images based on subtle echo signals without excessive noise present. Modern ultrasound systems have very sensitive transducers with a wide dynamic range. Of course, attenuation increases with range and this means that the ability to image deeper structures in the body is limited by the system sensitivity. This depth range may be affected by damage to the transducer, either to the elements themselves or to the matching layer that is the interface between the acoustic element and the body. Damage to the insulation surrounding the transducer cable may affect sensitivity due to the increased RF noise that is detected and amplified by the scanner electronics.

Phantoms are used to assess the sensitivity of the system by determining the maximum depth of penetration. An quasi-objective visual test is possible, where the observer uses the calipers to place a point at which the noise overcomes the echo signals. A more objective method is to use a computer to analyze the statistical properties of the image data and determine a merit factor that relates to signal versus noise [59].

Image uniformity is important for accurate diagnostic review by physicians. Non-uniformities in the image might be mistaken for pathology or artifacts related to pathology. Imaging of a known material, e.g., phantom with a uniform background, allows the end user to have confidence in the performance of the instrument. A uniform appearance across the lateral direction indicates that all elements of the transducer are performing nominally. Non-uniformity in the axial direction may be the result of an incorrect reconstruction with multiple transmit focus, defective time-gain amplification or errors in the transmit and receive focusing of the beam.

For a state-of-the-art ultrasound scanner, image uniformity is most likely to be caused by transducer damage or malfunction in a group of elements. A recent report cites image uniformity as the most likely issue to be discovered by routine quality control testing [60]. As a result, these authors recommended quarterly inspections of ultrasound units and transducers for image uniformity.

Ultrasound resolution, like the imaging systems, is complex. Spatial resolution can be thought of in terms of three dimensions, which are not isotropic and varying with the depth in the acoustic field (figure of ultrasound planes). Resolution in ultrasound imaging is closely related to frequency; generally, higher frequencies improve the spatial resolution. Contrast resolution could improve (in part because of changes in speckle), but higher attenuation usually defeats this improvement when deeper penetration is required. Multi-element transducers offer the potential to

improve spatial resolution through the use of wide apertures and time-delay focusing [61]. Early ultrasound phantoms presented a set of targets (nylon strings) to testing the axial and lateral spatial resolution only. Even then, the actual resolution measurement was neither truly all axial nor truly lateral, but rather a combination.

A group at the FDA introduced the concept of contrast and detail, after the same fashion used for computed tomography [8]. This phantom used targets of varying backscatter in the shape of cones to present different size “lesions” of varying contrast levels. An observer was to determine the minimum dimension and contrast that could be detected against the background. However, this arrangement assumes that the targets encountered by an ultrasound system are essentially two-dimensional. Further complicating matters is the use of various image scaling and interpolation algorithms, applied to real-time image display. This, combined with adjustable gain, makes evaluation of spatial resolution a difficult proposition [62].

The introduction of multi-row transducers made possible focusing of the beam in the elevational plane. This improves spatial resolution and, due to the lessening of partial volume artifact, improves contrast resolution. Madsen and Rownd proposed a phantom to test spatial resolution based on the ability to visualize spherical objects with no scattering against a background with identical sound speed and attenuation [63]. This phantom, in combination with a computer assisted analysis, provides an objective means by which spatial resolution could be determined [64–66].

9.9 Doppler Phantoms

Doppler ultrasound applications have existed as long as ultrasound imaging. Beginning with continuous wave Doppler, the introduction of duplex Doppler and color flow imaging in the 1980s and 1990s has led to the development of phantoms to assess performance and quantitative accuracy [13, 67–69].

Doppler phantoms are either built with a mechanical device for presenting motion to the ultrasound beam or are built with a pump system and simulated vessels in a TM background (vessel-based phantoms which shall be referred to as VB phantoms). The advantage of the former is that calibration of velocity is simple and accurate. These types of phantoms do not, however, challenge the signal to noise limits of the Doppler ultrasound system. The VB phantoms, while not provided a precisely calibrated velocity, provide a more realistic test of the Duplex and color flow systems. As previously discussed, the echogenicity of blood is low compared to soft tissues. Blood-mimicking fluids have been the topic of a number of publications; however, one physical aspect of blood that is very difficult to reproduce is the non-Newtonian property of blood. This affects the flow profile in both normal and stenotic vessels.

The pulsatile flow of blood as a result of normal cardiac contraction has been modeled in phantoms. This is a goal that developers have tried to achieve due in part to the importance of waveform peak and minimum velocities on the computation of flow indices [70]. Simple pumping systems can only provide simple

flow patterns (constant or on/off). Various types of pumps have been proposed and built; these range in sophistication from a gravity flow system to typical pumping systems as well as a pump system specially built to mimic cardiac flow [71]. Collaboration between groups involved in CT and MRI may also prove useful to developing more realistic pulsatile flow patterns.

VB phantoms range from simple arrangements of tubes to sophisticated models of pathology. The latter are often modeled after mild to severe stenoses [72–74] of the common carotid artery including the branch into the internal and external carotid arteries [74, 75]. In addition, some phantoms have been built to demonstrate low flow rate in very small bundles, as a means to evaluate the ability to detect perfusion with power Doppler systems [76, 77].

9.9.1 Current/Future Developments

Current ultrasound phantoms designed for quality control testing are evolving in response to more recent developments in ultrasound technology. Maintaining good contact and acoustic coupling is one problem encountered during the testing of curvilinear transducers. Working groups within the American Association of Physicists in Medicine [78], the International Electrotechnical Commission [79], and the American Institute of Ultrasound in Medicine [80] continue to work on modifications to the phantom design to accommodate these and other probes. A similar type of issue is encountered with the introduction of full two-dimensional arrays. In this situation, the acoustic window of the phantom needs to be of the proper size to have the transducer fit. Along with the efforts to develop these phantoms, a number of various groups are working on computer programs designed to work with one or more ultrasound phantoms to provide objective performance measurements.

Efforts to develop a standard ultrasound accreditation phantom have been difficult; however, there is ongoing work at the American College of Radiology to develop a required set of tests and performance measures for both the Ultrasound Accreditation Program and the Breast Ultrasound Accreditation Program. While not currently in the plans, an accreditation phantom standard would be of benefit to make testing procedures uniform and allow performance measures to be used in a manner similar to that for mammography, CT, and MRI accreditation programs.

Another area of development has been the electronic based “phantoms.” In these, there is no tissue-mimicking material involved. Rather, electronic transducers couple to the ultrasound scanner probe and “respond” to the pulsing by the scanner by “returning” controlled echo signals. One system involves a test of only the transducer, using compatible connector and a water tank to perform a pulse-receive test on each element of the probe (Fig. 9.8). This procedure allows one to detect individual elements which are in full or partial failure. This device is promoted as a tool to allow individual consultants or institutions to screen probes for proper functioning [81, 82]. This same concept (testing individual elements) is



Fig. 9.8 Example of an electronic ultrasound test device—the ultrasound transducer is mounted on the stand to the right and placed in a water tank. The probe is connected to the box on the left which is controlled by a computer. Individual “pings” of elements of the transducer produce echoes which bounce back from the reflector (this is configured for a curvilinear probe) and processed to determine which elements are operational

applied in a simpler device, which pings back when a pulse is detected. During the operation of this tool, the monitor of the ultrasound system is reviewed to visualize the response. If there is some dropout due to failed or malfunctioning elements, it would be visualized on the image. A similar approach has been implemented for at least one major ultrasound vendor through internal software available via a service interface.

Another form of electronic test phantom has been developed to test Doppler instruments [83]. Programming these electronic phantoms is considerably complex; however, once accomplished, there is a considerable flexibility to change the responding signal, for example, Doppler-shifted frequencies, additive noise, and varying levels of attenuation and speckle. Descriptions of these types of phantoms include an interface to a MATLAB program to allow for custom programming of the response to the transducer.

9.10 Summary

Ultrasound phantoms vary widely by application. The majority of phantoms constructed for sale are used in the quality control application whereas many of the in-house phantoms are fabricated by research groups to meet the experimental and development needs. In both cases, TM materials are most likely to be based on gelatin materials, from recipes that have been empirically found to control sound speed, attenuation, and backscatter.

Future phantom developments will most likely be required to match improvements in ultrasound system technology; ideally, these would include acoustic parameters of quantitative interest, both as a means of verifying proper machine operation as well as providing confidence in measurements made by the ultrasound system. As sophistication of ultrasound equipment increases, the demands for acoustically realistic materials and phantoms will likely also increase.

References

1. Carson, P. L., & Fenster, A. (2009). Anniversary paper: Evolution of ultrasound physics and the role of medical physicists and the AAPM and its journal in that evolution. *Medical Physics*, *36*, 411–428.
2. Madsen, E. L., Zagzebski, J. A., Banjavic, R. A., & Jutila, R. E. (1978). Tissue mimicking materials for ultrasound phantoms. *Medical Physics*, *5*, 391–394.
3. Burlew, M. M., Madsen, E. L., Zagzebski, J. A., Banjavic, R. A., & Sum, S. W. (1980). A new ultrasound tissue-equivalent material. *Radiology*, *134*, 517–520.
4. Carson, P., & Zagzebski, J. A. (1980). *Pulse echo ultrasound imaging systems: Performance tests and criteria* (pp. 1–79). College Park, MD: AAPM.
5. Banjavic, R. A., & Zagzebski, J. A. (1981). Ultrasonic pulse-echo beam width and axial response approximations for clinical broadband focused transducers. *Ultrasound in Medicine and Biology*, *7*, 63–71.
6. Zagzebski, J. A., Banjavic, R. A., Madsen, E. L., & Schwabe, M. (1982). Focused transducer beams in tissue-mimicking material. *Journal of Clinical Ultrasound*, *10*, 159–166.
7. Madsen, E. L., Zagzebski, J. A., & Frank, G. R. (1982). An anthropomorphic ultrasound breast phantom containing intermediate-sized scatterers. *Ultrasound in Medicine and Biology*, *8*, 381–392.
8. Smith, S. W., & Lopez, H. (1982). A contrast-detail analysis of diagnostic ultrasound imaging. *Medical Physics*, *9*, 4–12.
9. Sheppard, J., & Duck, F. A. (1982). Ultrasonic tissue-equivalent materials using inorganic gel mixtures. *British Journal of Radiology*, *55*, 667–669.
10. van Wijk, M. C., & Thijssen, J. M. (2002). Performance testing of medical ultrasound equipment: fundamental vs. harmonic mode. *Ultrasonics*, *40*, 585–591.
11. Oudry, J., Bastard, C., Miette, V., Willinger, R., & Sandrin, L. (2009). Copolymer-in-oil phantom materials for elastography. *Ultrasound Medical Biology*, *35*, 1185–1197 (2009). [pii]:S0301-5629(09)00053-2, doi:[10.1016/j.ultrasmedbio.2009.01.012](https://doi.org/10.1016/j.ultrasmedbio.2009.01.012).
12. Bridal, S. L., Roberjot, V., Laugier, P. & Berger, G. (1996). Attenuation and backscatter coefficient measurements from 2 to 60 MHz using backscattered RF signals from a tissue-mimicking phantom. In *Proceedings of the IEEE Ultrasonics Symposium 2*, (pp. 1151–1154).
13. Kollmann, C., Bezemer, R. A., Fredfeldt, K. E., Schaarschmidt, U. G. & Teirlinck, C. J. in *Ultraschall in der Medizin* (Stuttgart, Germany: 1980) Vol. 20, (pp. 248–257, 1999).
14. Kollmann, C. in *Ultraschall in der Medizin* (Stuttgart, Germany : 1980) Vol. 28, (pp. 438–439, 2007).
15. Nadkarni, S. K., Austin, H., Mills, G., Boughner, D., & Fenster, A. (2003). A pulsating coronary vessel phantom for two-and three-dimensional intravascular ultrasound studies. *Ultrasound in Medicine and Biology*, *29*(4), 621–628.
16. Rickey, D. W. & Fenster, A. A. (1996). Doppler ultrasound clutter phantom. *Ultrasound in Medicine and Biology*, *22*, 747–766 (1996). [pii]:0301562996000452.
17. Insana, M., Zagzebski, J., & Madsen, E. (1983). Improvements in the spectral difference method for measuring ultrasonic attenuation. *Ultrasonic Imaging*, *5*, 331–345.

18. Insana, M. F., Madsen, E. L., Hall, T. J., & Zagzebski, J. A. (1986). Tests of the accuracy of a data reduction method for determination of acoustic backscatter coefficients. *Journal of the Acoustical Society of America*, 79, 1230–1236.
19. Hall, T. J., Madsen, E. L., Zagzebski, J. A., & Boote, E. J. (1989). Accurate depth-independent determination of acoustic backscatter coefficients with focused transducers. *Journal of the Acoustical Society of America*, 85, 2410–2416.
20. Wear, K. A. et al. (2005). Interlaboratory comparison of ultrasonic backscatter coefficient measurements from 2 to 9 MHz. *Journal of Ultrasound in Medicine*, 24, 1235–1250 (2005). [pii]:24/9/1235.
21. Stiles, T. A., Madsen, E. L., Frank, G. R., Diehl, T. & Lucey, J. A. Tissue-mimicking liquid for use in exosimetry. *Journal of Ultrasound in Medicine*, 24, 501–516 (2005). [pii]:24/4/501.
22. Insana, M. F., Hall, T. J., Chaturvedi, P., & Kargel, C. (2001). Ultrasonic properties of random media under uniaxial loading. *Journal of the Acoustical Society of America*, 110, 3243–3251.
23. Auntminnie. (2012). Study: Global ultrasound market to grow at 5% rate. <http://www.auntminnie.com/index.aspx?sec=ser&sub=def&pag=dis&ItemID=98757>.
24. IEC-Technical-Committee-87. (2011). Ultrasonics—Real-time pulse-echo scanners—Phantom with cylindrical, artificial cysts in tissue-mimicking material and method for evaluation and periodic testing of 3D-distributions of void-detectability ratio (VDR). <http://webstore.iec.ch/webstore/webstore.nsf/artnum/044952!opendocument>.
25. IEC-Technical-Committee-87. (1986). Methods of measuring the performance of ultrasonic pulse-echo diagnostic equipment. <http://webstore.iec.ch/webstore/webstore.nsf/artnum/017421!opendocument>.
26. King, D. M., Hangiandreou, N. J., Tradup, D. J. & Stekel, S. F. (2010). Evaluation of a low-cost liquid ultrasound test object for detection of transducer artefacts. *Physics in Medicine and Biology*, 55, N557–N570 (2010). [pii]:S0031-9155(10)59794-X, doi:10.1088/0031-9155/55/23/N01.
27. Lo, M. D., Ackley, S. H. & Solari, P. (2012). Homemade ultrasound phantom for teaching identification of superficial soft tissue abscess. *Emergency Medicine Journal*, 29, 738–741 (2012). [pii]:emermed-2011-200264, doi:10.1136/emermed-2011-200264.
28. Browne, J. E., Ramnarine, K. V., Watson, A. J. & Hoskins, P. R. Assessment of the acoustic properties of common tissue-mimicking test phantoms. *Ultrasound in Medicine and Biology*, 29, 1053–1060 (2003). [pii]:S030156290300053X.
29. Hoskins, P. R. (2008). Simulation and validation of arterial ultrasound imaging and blood flow. *Ultrasound in Medicine and Biology*, 34, 693–717 (2008). [pii]:S0301-5629(07)00549-2, doi:10.1016/j.ultrasmedbio.2007.10.017.
30. Cannon, L. M., Fagan, A. J. & Browne, J. E. (2011). Novel tissue mimicking materials for high frequency breast ultrasound phantoms. *Ultrasound in Medicine and Biology*, 37, 122–135 (2011). [pii]:S0301-5629(10)00537-5, doi:10.1016/j.ultrasmedbio.2010.10.005.
31. Culjat, M. O., Goldenberg, D., Tewari, P. & Singh, R. S. (2010). A review of tissue substitutes for ultrasound imaging. *Ultrasound in Medicine and Biology*, 36, 861–873 (2010). [pii]:S0301-5629(10)00075-X, doi:10.1016/j.ultrasmedbio.2010.02.012.
32. Brewin, M. P., Pike, L. C., Rowland, D. E. & Birch, M. J. (2008). The acoustic properties, centered on 20 MHz, of an IEC agar-based tissue-mimicking material and its temperature, frequency and age dependence. *Ultrasound in Medicine and Biology*, 34, 1292–1306 (2008). [pii]:S0301-5629(07)00661-8, doi:10.1016/j.ultrasmedbio.2007.12.017.
33. AIUM. (1975). The AIUM 100 mm test object and recommended procedures for its use. *Reflections*, 1, 74–91.
34. Lubbers, J. (1998). *Ultrasound in Medicine and Biology*.
35. Madsen, E. L., Frank, G. R. & Dong, F. Liquid or solid ultrasonically tissue-mimicking materials with very low scatter. *Ultrasound in Medicine and Biology*, 24, 535–542 (1998). [pii]:S0301-5629(98)00013-1.

36. Ramnarine, K. V., Nassiri, D. K., & Hoskins, P. R. (1998). Validation of a new blood-mimicking fluid for use in Doppler flow test objects. *Ultrasound in Medicine and Biology*, *24*, 451–459.
37. Browne, J. E., Watson, A. J., Hoskins, P. R., & Elliott, A. T. (2005). Investigation of the effect of subcutaneous fat on image quality performance of 2D conventional imaging and tissue harmonic imaging. *Ultrasound in Medicine and Biology*, *31*, 957–964.
38. Madsen, E. L., et al. (2006). Anthropomorphic breast phantoms for testing elastography systems. *Ultrasound in Medicine and Biology*, *32*, 857–874.
39. Parker, K. J., Dooley, M. M. & Rubens, D. J. (2011). Imaging the elastic properties of tissue: the 20 year perspective. *Physics in Medicine and Biology*, *56*, R1–R29 (2011). [pii]:S0031-9155(11)64279-0, doi:[10.1088/0031-9155/56/1/R01](https://doi.org/10.1088/0031-9155/56/1/R01).
40. Teirlinck, C. J., et al. (1998). Development of an example flow test object and comparison of five of these test objects, constructed in various laboratories. *Ultrasonics*, *36*, 653–660.
41. Kondo, T., & Kitatuji, M. (2005). New tissue mimicking materials for ultrasound phantoms. *Ultrasonics Symposium*, *3*, 1664–1667.
42. Nicholas, D. (1982). Evaluation of backscattering coefficients for ex-cised human tissues: Results interpretation and associated measurements. *Ultrasound in Medicine and Biology*, *8*, 17–28.
43. Bamber, J. C., & Hill, C. R. (1981). Acoustic properties of normal and cancerous human liver—I. dependence on pathological condition. *Ultrasound in Medicine and Biology*, *7*, 121–133.
44. Sleefe, G. E., & Lele, P. P. (1988). Tissue characterization based on scatterer number density estimation. *IEEE Transactions on Ultrasonics, Ferroelectrics and Frequency, Control*, *35*, 749–757. doi:[10.1109/58.9332](https://doi.org/10.1109/58.9332).
45. Ophir, J., Céspedes, I., Ponnekanti, H., Yazdi, Y., & Li, X. (1991). Elastography: A quantitative method for imaging the elasticity of biological tissues. *Ultrasonic Imaging*, *13*, 111–134.
46. Hall, T. J. (2003). AAPM/RSNA physics tutorial for residents: topics in US: Beyond the basics: Elasticity imaging with US. *Radiographics*, *23*, 1657–1671 (2003). [pii]:23/6/1657, doi:[10.1148/rg.236035163](https://doi.org/10.1148/rg.236035163).
47. Walker, W. F., Fernandez, F. J., & Negron, L. A. (2000). A method of imaging viscoelastic parameters with acoustic radiation force. *Physics in Medicine and Biology*, *45*, 1437–1447.
48. Nightingale, K. R., Palmeri, M. L., Nightingale, R. W., & Trahey, G. E. (2001). On the feasibility of remote palpation using acoustic radiation force. *Journal of the Acoustical Society of America*, *110*, 625–634.
49. Sommer, F. G., Filly, R. A., Edmonds, P. D., Reyes, Z., & Comas, M. E. (1980). A phantom for imaging biological fluids by ultrasound and CT scanning. *Ultrasound in Medicine and Biology*, *6*, 135–140.
50. Blechinger, J. C., Madsen, E. L., & Frank, G. R. (1988). Tissue-mimicking gelatin-agar gels for use in magnetic resonance imaging phantoms. *Medical Physics*, *15*, 629–636.
51. D’Souza, W. D., et al. (2001). Tissue mimicking materials for a multi-imaging modality prostate phantom. *Medical Physics*, *28*, 688–700.
52. Lee, Y. C., Fullerton, G. D., Baiu, C., Lescrenier, M. G., & Goins, B. A. (2011). Preclinical multimodality phantom design for quality assurance of tumor size measurement. *BMC Medical Physics*, *11*, 1.
53. Hipp, E., Partanen, A., Karczmar, G. S., & Fan, X. (2012). Safety limitations of MR-HIFU treatment near interfaces: A phantom validation. *Journal of Applied Clinical Medical Physics*, *13*, 3739.
54. Shevchenko, N., Schwaiger, J., Markert, M., Flatz, W. & Lueth, T. C. Evaluation of a resectable ultrasound liver phantom for testing of surgical navigation systems. In *IEEE Annual International Conference of the Engineering in Medicine and Biology Society 2011*, (pp. 916–919). doi:[10.1109/IEMBS.2011.6090205](https://doi.org/10.1109/IEMBS.2011.6090205).
55. Anon. Saran (plastic). [http://en.wikipedia.org/wiki/Saran_\(plastic\)](http://en.wikipedia.org/wiki/Saran_(plastic)).

56. Xu, D., Abbas, S. & Chan, V. W. (2005). Ultrasound phantom for hands-on practice. *Regional Anesthesia and Pain Medicine*, 30, 593–594 (2005). [pii]:S1098-7339(05)00539-0, doi:10.1016/j.rapm.2005.08.007.
57. McCarty, K., & Stewart, W. (1983). Aspects of the design of performance measuring test objects. *Ultrasound in Medicine and Biology*, Suppl 2, 185–189.
58. Goodsitt, M. M., Carson, P. L., Witt, S., Hykes, D. L., & Kofler, J. M., Jr. (1998). Real-time B-mode ultrasound quality control test procedures. Report of AAPM Ultrasound Task Group No. 1. *Medical Physics*, 25, 1385–1406.
59. Thijssen, J. M., Weijers, G., & de Korte, C. L. (2007). Objective performance testing and quality assurance of medical ultrasound equipment. *Ultrasound in Medicine and Biology*, 33, 460–471.
60. Hangiandreou, N. J., Stekel, S. F., Tradup, D. J., Gorny, K. R. & King, D. M. (2011). Four-year experience with a clinical ultrasound quality control program. *Ultrasound in Medicine and Biology*, 37, 1350–1357 (2011). [pii]:S0301-5629(11)00250-X, doi:10.1016/j.ultrasmedbio.2011.05.007.
61. Thomenius, K. (1996). Evolution of ultrasound beamformers. In *Proceedings of IEEE Ultrasonics Symposium*, Vol. 2, (pp. 1615–1622).
62. Kanal, K. M., Kofler, J. M., & Groth, D. S. (1998). Comparison of selected ultrasound performance tests with varying overall receiver gain and dynamic range, using conventional and magnified field of view. *Medical Physics*, 25, 642–647.
63. Rownd, J. J., Madsen, E. L., Zagzebski, J. A., Frank, G. R. & Dong, F. (1997). Phantoms and automated system for testing the resolution of ultrasound scanners. *Ultrasound in Medicine and Biology*, 23, 245–260 (1997). [pii]:S0301562996002050.
64. Kofler, J. M., Jr. & Madsen, E. L. (2001). Improved method for determining resolution zones in ultrasound phantoms with spherical simulated lesions. *Ultrasound in Medicine and Biology*, 27, 1667–1676 (2001). [pii]:S0301562901004732.
65. Kofler, J. M., Lindstrom, M. J., Kelcz, F., & Madsen, E. L. (2005). Association of automated and human observer lesion detecting ability using phantoms. *Ultrasound in Medicine and Biology*, 31, 351–359.
66. Kofler, J. M., & Madsen, E. L. (2002). Improved method for determining resolution zones in ultrasound phantoms with spherical simulated lesions. *Ultrasound in Medicine and Biology*, 27, 1667–1676.
67. Hoskins, P. R., Anderson, T., & McDicken, W. N. (1989). A computer controlled flow phantom for generation of physiological Doppler waveforms. *Physics in Medicine and Biology*, 34, 1709–1717.
68. Stewart, S. F. (2001). Effects of transducer, velocity, Doppler angle, and instrument settings on the accuracy of color Doppler ultrasound. *Ultrasound in Medicine and Biology*, 27, 551–564.
69. Boote, E. J., & Zagzebski, J. A. (1988). Performance tests of Doppler ultrasound equipment with a tissue and blood-mimicking phantom. *Journal of Ultrasound in Medicine*, 7, 137–147.
70. Thompson, R. S., Trudinger, B. J., & Cook, C. M. (1988). Doppler ultrasound waveform indices: A/B ratio, pulsatility index and Pourcelot ratio. *British Journal of Obstetrics and Gynaecology*, 95, 581–588.
71. Rickey, D. W., Rankin, R., & Fenster, A. (1992). A velocity evaluation phantom for colour and pulsed Doppler instruments. *Ultrasound in Medicine and Biology*, 18, 479–494.
72. Rickey, D. W., Picot, P. A., Christopher, D. A. & Fenster, A. (1995). A wall-less vessel phantom for Doppler ultrasound studies. *Ultrasound in Medicine and Biology*, 21, 1163–1176 (1995). [pii]:0301562995000445.
73. Guo, Z. & Fenster, A. (1996). Three-dimensional power Doppler imaging: a phantom study to quantify vessel stenosis. *Ultrasound in Medicine and Biology*, 22, 1059–1069 (1996). [pii]:S0301562996001251.
74. Grant, E. G. et al. (2003). Carotid artery stenosis: Gray-scale and Doppler US diagnosis—society of radiologists in ultrasound consensus conference. *Radiology*, 229, 340–346 (2003). [pii]:2292030516, doi:10.1148/radiol.2292030516.

75. King, D. M., Ring, M., Moran, C. M., & Browne, J. E. (2010). Development of a range of anatomically realistic renal artery flow phantoms. *Ultrasound in Medicine and Biology*, *36*, 1135–1144. (Elsevier Ltd, 2010).
76. Gessner, R. C., Kothadia, R., Feingold, S. & Dayton, P. A. (2011). 3-D microvessel-mimicking ultrasound phantoms produced with a scanning motion system. *Ultrasound in Medicine and Biology*, *37*, 827–833 (2011). doi:S0301-5629(10)00676-9 [pii] [10.1016/j.ultrasmedbio.2010.12.013](https://doi.org/10.1016/j.ultrasmedbio.2010.12.013).
77. Hindle, A. J., & Perkins, A. C. (1994). A perfusion phantom for the evaluation of ultrasound contrast agents. *Ultrasound in Medicine and Biology*, *20*, 309–314.
78. American Association of Physicists in Medicine. www.aapm.org.
79. International Electrotechnical Commission.
80. American Institute of Ultrasound in Medicine.
81. Weigang, B., Moore, G., Gessert, J., & Phillips, W. (2003). The methods and effects of transducer degradation on image quality and the clinical efficacy of diagnostic sonography. *Journal of Diagnostic Medical Sonography*, *19*, 3–13.
82. Mårtensson, M., Olsson, M., & Brodin, L. Å. (2010). Ultrasound transducer function: annual testing is not sufficient. *European Journal of Echocardiography*, *11*(9), 801–805.
83. Gittins, J. & Martin, K. (2010). The Leicester Doppler phantom—a digital electronic phantom for ultrasound pulsed Doppler system testing. *Ultrasound in Medicine and Biology*, *36*, 647–655 (2010). doi:10.1016/j.ultrasmedbio.2010.01.003.